Amorphous Materials for Micrometer and Submicrometer Bubble Domain Technology

Abstract: A review and critique is made of those material and processing issues that pertain to the implementation of micrometer and submicrometer bubble devices on amorphous films. Adequate reproducibility and uniformity have been achieved in ternary amorphous films prepared by rf sputtering and their magnetic characteristics are very similar to those of analogous garnet films. Factors that may limit application to the amorphous films include defects and dielectric breakdown in insulating layers, sensitivity to annealing, and larger, but not prohibitive, coercivities. A salient problem common to both garnet and amorphous materials is attainment of sufficiently large values of Q to ensure stable device operation.

Introduction

To decrease storage costs its is clear that bubble devices will have to achieve high bit densities (10⁷ to 10⁸ bits/cm²), necessitating small-diameter bubbles in the micrometer range with a compatible lithography [1]. The smaller domain sizes impose critical demands on all the materials and processes used in a complete device. These demands call for innovative solutions to problems such as retention of optimized magnetic properties in the bubble media, lower defect levels in thinner films, and adequate dielectric breakdown strength, electromigration resistance, heat dissipation, mechanical fatigue, uniformity, etc. Strictly speaking, these problems are not new. The technology for smaller bubble sizes, however, requires that the materials operate reliably near their ultimate limits.

At present the two leading contenders for the storage layer are epitaxial garnet films and amorphous films that are alloys of rare earths and the transition metals. Historical factors have led to a well established and advanced level of development of garnet films, but with primary emphasis on films capable of supporting bubbles of relatively large diameter (3 to $10~\mu m$). Achievement of micrometer and submicrometer diameters requires substantial modification of film properties, and hence film compositions and growth techniques, relative to those used in the past. By contrast, amorphous films have evolved more recently and have been characterized less comprehensively than garnet films.

In this paper we define the critical material and processing issues required to implement micrometer and submicrometer bubble devices on amorphous films. We primarily emphasize questions concerning the storage films. The issues of lithography, overlay metallurgy, dielectric spacers, processing of the latter, and the design, packaging, and operation of complete devices [2] are discussed only to the extent that these impose special requirements on the storage films and substrates available for these objectives. Where appropriate, amorphous film properties are compared with those of analogous garnet films. One of our main objectives is an up-to-date summary of the state of the art in this field, encompassing previously published subjects, as well as results from our work. Most of the latter consist of previously unpublished data on film deposition procedures, film composition design, attainment of desirable properties, reproducibility, anisotropy, domain stability, and coercivity.

For up-to-date information on garnet film materials, the reader is referred to a review article by Davies and Giess [3] and to the special issue of the *Journal of Crystal Growth*, volume 27, which contains a paper by Robertson et al. [4], where films produced by vertical dipping are discussed.

General considerations

This section summarizes several special requirements that must be satisfied to successfully implement micrometer and submicrometer devices. These criteria are used to assess the amorphous films in subsequent sections.

• Submicrometer physics and device requirements Ideally, bubble films should approximately satisfy the criteria developed by Thiele [5, 6] and others. These may be summarized as follows:

1. For the existence of stable bubble domains, the material must have a unique easy axis of magnetization perpendicular to the plane of the film such that the stability factor Q is greater than unity, where

$$Q = K/2\pi M^2 > 1. \tag{1}$$

In Eq. (1), K is the uniaxial anisotropy energy density and M is the magnetization. Although Q > 1 may allow for stable bubbles in a film, consideration of the need to propagate the bubbles without spurious nucleation of unwanted bubbles in actual devices calls for Q's in excess of approximately 2.5 [7].

- 2. Maximum stability of a bubble is reached when the film thickness h equals approximately $\frac{1}{2}$ of the bubble diameter d.
- 3. With the constraint cited in 2), the bubble diameter is given by

$$d \approx 8l$$
.

where
$$l = (AK)^{\frac{1}{2}} / \pi M^2 = (2AQ/\pi)^{\frac{1}{2}} / M,$$
 (2)

in which A is the material exchange constant and l defines the characteristic material length, the ratio of wall energy to magnetostatic demagnetizing energy.

- 4. In general, minimizing the power required to propagate the bubbles requires minimizing the coercivity H_c . However, in T-I bar type devices the lowest practical rotating field for bubble propagation depends strongly on M as a result of interbar gaps [8, 9]. Thus propagating power is negligibly increased even if H_c is as large as one percent of $4\pi M$. But in contiguous disk devices [10] that do not have gaps, and bubble lattice devices [11] that propagate bubbles by means of bubble-bubble interactions, it is always desirable to use films with the lowest achievable coercivities.
- Since the minimum propagation field in T-1 bar devices is proportional to M, it is desirable to minimize
 M while satisfying the other relations.

Referring to Eq. (2), we note that reducing bubble diameter requires adjustment of A, K, and M. The minimum exchange constant is established by considerations of temperature sensitivity. It must be sufficiently large to ensure a Curie temperature well in excess of 100° C. Bubble stability requires that Q > 2.5 [7]. The 5- μ m materials discussed subsequently possess Q's in the range 5 to 10, leaving some room for decreasing Q. However, further consideration of these two constraints suggests that achieving bubbles much smaller than 5 μ m generally requires that both M and K be larger than those of 5- μ m materials. It is not clear whether these adjustments and limits can be achieved in all garnet and amorphous materials.

All of these parameters generally vary with film composition, growth conditions, and ambient temperature.

A complete assessment of a film material requires understanding of all these dependences. However, these parameters establish several critical fields, such as the bubble collapse and stripe-out fields, which can be directly correlated with the operating margins of a complete device [12]. It is therefore more practical to use such fields as a measure of the suitability of a storage film. Specifically, the temperature sensitivity, as well as uniformity and reproducibility of film properties, can be conveniently assessed by measuring the temperature dependence, uniformity, and reproducibility of the stripe-collapse field $H_{\rm sc}$ and the stripe width $w_{\rm s}$.

Film deposition processes for dielectric layers and propagation/conductor overlays often require substrate temperatures as high as 250°C. Assembly of wafers into a practical package with many serial electrical connections may require a solder hierarchy over a 150° to 250°C range. These considerations suggest that all film components in a device, including the bubble medium, be capable of withstanding short term exposures to approximately 250°C.

Consideration of realistic device operating environments and Joule heating in conductors suggests that films maintain integrity of data over a temperature range of approximately 0° to 100°C. A monotonic change in operating margins with temperature can be in part compensated by changing the relevant bias and propagation fields with temperature. Straightforward provision of bias field compensation with ordinary permanent magnets, and consideration of typical operating margins, suggest that the stripe collapse field can change, preferably decrease, by as much as 20 percent over a 100°C increase above room temperature.

Processing throughput and efficient packaging of any bubble device make it desirable to maximize substrate dimensions while maintaining adequate uniformity over most of this area. Similar considerations call for stringent tolerances on reproducibility of all relevant storage film properties. A device operating margin of 20 percent suggests a tolerance for reproducibility and uniformity of stripe collapse field of \pm two percent. Since T-I bar type devices can tolerate a 3/1 bubble diameter range between the lower and upper bias margins, the stripe width tolerance can be as liberal as \pm ten percent. The latter is easily met in films with the collapse field tolerances mentioned previously.

• Substrate requirements

Practical considerations dictate the use of large-area, rigid substrates having a high degree of surface smoothness. Epitaxial garnet films, of course, require single-crystal garnet substrates. On the other hand, amorphous films can be deposited on a variety of surfaces. One attractive candidate for the amorphous film would seem

to be a glass substrate, since it can potentially meet stringent surface finish requirements at very low cost. However, consideration of power dissipation in the control lines necessary in current device configurations may require a substrate of higher thermal conductivity, such as silicon.

Table 1 summarizes estimates of the thermal excursions that can be expected within and in the vicinity of conductor lines of the type required in T-I bar type devices with bubble diameters in the one-micrometer range. The table gives comparative data for three types of substrates: garnet, glass, and silicon. These are calculated for an assumed current of 10 mA dc through an Au transfer line of dimension $0.5 \times 0.3 \times 2000$ micrometers on heat sunk substrates 0.5 mm thick, with 25 conductors/ cm². Note that this corresponds to a heat input of 2.5 W/cm², which on glass could easily cause a 100°C temperature rise in the vicinity of each conductor, which is about 10 to 100 times larger than on garnet and silicon, respectively. Since the thermal risetime of such lines can be as small as one μ s, such temperature excursions could occur under pulsed operation of actual devices. A 100°C temperature rise could adversely affect the stability of the domains under the conductors and could conceivably accelerate conductor failures by mechanical fatigue due to dissimilar thermal expansion coefficients in the conductor and the substrate.

The foregoing comparison suggests that a glass substrate is not an obvious choice for the amorphous film. In addition, conventional glass substrates are typically contaminated with glass debris from cutting operations, which is difficult to remove completely. This debris can be eliminated by lapping and polishing techniques. However, these operations substantially increase the cost of the glass substrate, making it comparable to the cost of polished silicon substrates of the type used in semiconductor applications which are presently available in 7.5- to 10-cm diameters. Silicon substrates, therefore, are likely to prevail for amorphous films.

• Dielectric breakdown

Bubble domain devices commonly employ an electrically insulating spacer between the storage film and the propagating/conductor overlays. The use of dielectric garnet films allows liberal requirements on the insulating characteristics of the spacer film. On the other hand, amorphous metal films are conductive and consequently can give rise to electric fields between the conductors and the film. A recent investigation of this problem established the fact that sputtered SiO_2 films are one of the preferred choices and can reliably withstand electric fields smaller than $6\times10^5~\mathrm{V/cm}$ [13]. This corresponds to a maximum voltage of six volts across 1000 Å spacers, values that are likely to be required in most devices with

Table 1 Calculations of thermal conductivity and temperature rise to be expected in 1- μ m bubble devices in the vicinity of each conductor.^a

Substrate	Thermal conductivity $(W/cm - K)$	ΔT (°C)
Si	1.30	1
Garnet	0.08	16
Glass	0.01	130

^a0.5-mm thick substrates with heat sink; 0.5- μ m × 0.3- μ m × 2000- μ m Au lines; I = 10 mA, $J = 6 \times 10^6$ A/cm².

one-micrometer diameter bubbles. Everything else being equal, we feel that dielectric breakdown is the salient factor that may inhibit the application of the amorphous film.

Gd-Co-Mo film composition design

The observation of bubble domains in amorphous films and first-order characterization of their properties have been described in several previous publications [14-17].

Initially, binary films sputtered from Gd-Co targets were examined [14-16]. Investigation of their properties revealed that, although Gd-Co films could be made to support a broad range of bubble diameters at room temperature, they possessed unacceptably large saturation magnetizations, requiring excessively large rotating field amplitudes in T-I bar type devices, and also exhibited an unacceptably large variation of properties with temperature.

These deficiencies led to the development of ternary Gd-Co-X film compositions [17]. The type and quantity of the third constituent were chosen and adjusted to minimize both the magnetization at all bubble diameters and the temperature dependence of critical film properties. Au, Cu, Mo [17], and Cr [18] are among the additives investigated in some detail. The lack of a sound theoretical, analytical, and empirical background on these alloys, particularly in the amorphous state, has required extensive experimental assessment of their film properties. Progress in assessing broad ranges of compositions by sputtering has been difficult because of the limited number of compositions that can be achieved with one alloyed target. The latter limitation has been partly ameliorated, however, by the use of "mosaic" type binary targets (Gd segments on an Fe or Co base) [19, 20].

The gradual evolution of a data base has recently provided a semiquantitative analytical model [21, 22], based on molecular field considerations, which has been useful for predicting how some film properties (exchange constant, transition temperatures, and temperature de-

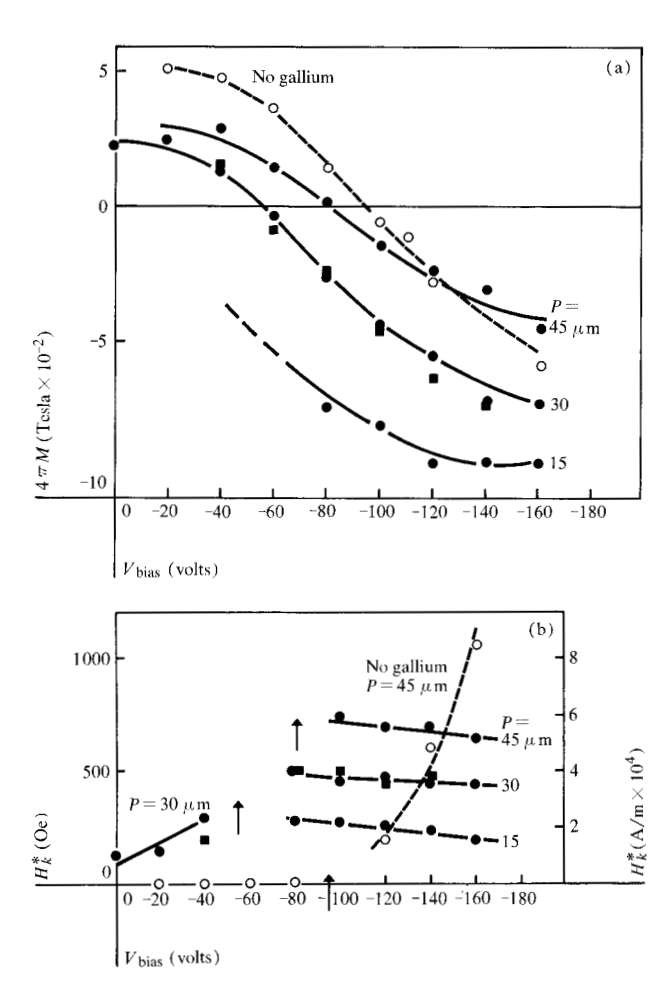


Figure 1 Dependence of composition and magnetic properties of Gd-Co-Mo films on sputtering parameters. (a) Magnetization vs bias voltage, with Ar pressure as a parameter. Solid circles are points for substrates backed with gallium, open circles for substrates without gallium backing, and squares for substrates backed with gallium but prepared on another system. (b) Effective anisotropy vs bias voltage, with Ar pressure as a parameter. Points are coded as in (a).

pendence of magnetization) depend on small changes in film composition. This model eases the task of predicting an "optimum" film composition from limited experimental data. Furthermore, the evaluation of new alloy systems has been recently expedited by three-source electron gun evaporation [23, 24], obviating the need for preparation of the restrictive single composition targets used in sputtering. Films with bubble domain characteristics have also been prepared by evaporation but in smaller quantities and with limited characterization [23, 24]. In principle either deposition process is potentially viable, and substantial additional work will be required to make a technical selection possible.

A salient gap in the knowledge about amorphous [15, 16] and garnet [25] film properties has been a mar-

ginal understanding of the mechanism that gives rise to their perpendicular magnetic anisotropy. This paper presents a detailed assessment of the anisotropy over a limited composition range in the Gd-Co-Mo system. To date there is no quantitative model for the anisotropy as a function of film composition, deposition method, or deposition conditions.

One alloy system that has been most broadly characterized and also appears to have a favorable combination of properties for micrometer and submicrometer applications is the Gd-Co-Mo ternary alloy. The remainder of this section therefore addresses targets, film compositions, and the sputtering process for Gd-Co-Mo films, although many of these considerations do apply as well to other alloys and other deposition methods.

As indicated in previous publications, the first sputtered amorphous films were prepared with arc-melted targets [14-18]. The target fabrication process consists in first alloying individual ingots of the desired constituents into binary or ternary ingots of the nominal target composition. An array of such ingots is melted in a suitable target base-plate, typically a Mo boat 12 to 25 cm in diameter. The individual alloy and target ingots are all melted in an electric arc furnace in high-purity Ar gas. The use of high-purity starting materials and the minimization of their contamination during handling and melting has resulted in a viable process for making experimental targets.

However, most alloys of rare earths and transition metals form complex intermetallics [26]. Thus are melting, although straightforward for melting the nominal compositions, typically results in large gradients in composition through the target thickness and across its planar dimensions. Accordingly, films sputtered onto a stationary array of substrates can exhibit unacceptably large nonuniformities of most film properties. For example, targets and stationary substrates 12 to 20 cm in diameter can result in 10:1 variations in stripe width over comparable dimensions in the substrate plane.

One way to improve the uniformity of the sputtered films is to rotate the substrate holder [27]. Simple rotation, however, does not eliminate radial inhomogeneities. The influence of target and plasma inhomogeneities can be minimized with a more complex substrate motion. This complication can be avoided by using hot-pressed targets, which can be made to have excellent long-wavelength uniformity, and by choosing sputtering geometries with adequately large aspect ratios.

We have recently evaluated hot-pressed targets for this application and established that these yield films with properties indistinguishable from those prepared from analogous arc-melted targets, except that the former eliminate the need for substrate rotation, simplifying the sputtering hardware, and providing uniformity limited

only by geometry. The films described here, however, were prepared from arc-melted targets over a rotating substrate holder.

The magnetic properties of sputtered Gd-Co-Mo films are strongly dependent on composition. Selecting an optimum composition requires satisfying the constraints outlined in the section entitled "General Considerations." Since at present little is known about the source and the magnitude of the anisotropy in this class of materials, their composition is first selected to minimize their room-temperature magnetization in conjunction with a small temperature dependence of bubble collapse field as required to achieve device operating margins that are insensitive to temperature. This temperature behavior can be obtained by selecting a composition with Curie and compensation temperatures equally spaced above and below room temperature. The use of limited empirical information and the molecular field analysis [21] can readily define a first-order composition. Further refinement of the composition requires a more timeconsuming empirical optimization of the perpendicular anisotropy and the temperature dependence of the characteristic length *l* (the bubble diameter).

As discussed below, the film composition is not necessarily the same as that of the target, so that additional correlation between film and target compositions is required. The model and this iterative approach have been successfully used to define a nearly optimum composition for micrometer bubbles in the Gd-Co-Mo system [22]. In essence the model predicts that achievement of "good" temperature insensitivity will be difficult for the Gd-Co-Mo compositions needed for 2- μ m bubbles or larger, but appears promising for micrometer and submicrometer film compositions. As suggested in this discussion, however, such an iterative approach is complex and has not allowed for rigorous definition and assessment of many alternate alloys.

Sputtering process for Gd-Co-Mo films

The rf sputtering process and hardware used for making these films has been amply described in the context of many thin film materials [28, 29], including the alloys of rare-earths and transition metals [27]. The critical dependences of composition and magnetic properties on sputtering parameters are summarized in Figs. 1 and 2.

Figure 1(a) is a plot of magnetization vs bias voltage at the Mo substrate holder, with the absolute Ar pressure as a parameter. The target composition is 67.5 at.% Co, 17.5 at.% Gd, and 15 at.% Mo. The spontaneous dc target voltage was held constant at -1200 V. For a target 13 cm in diameter with a target-to-substrate distance of 4 cm, these conditions correspond to approximately 100 W of power dissipated in the plasma. The indicated target and substrate voltages are established by tuning

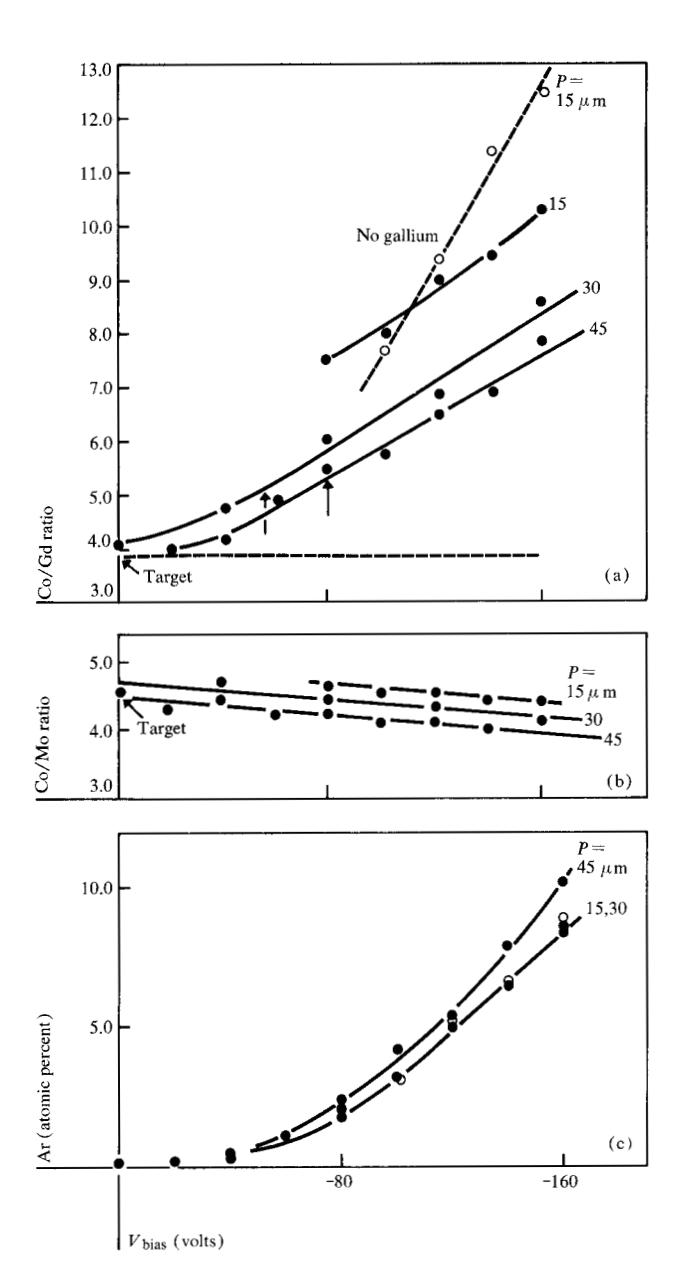


Figure 2 Film composition of Gd-Co-Mo films as a function of substrate bias voltage, with Ar pressure as a parameter. Bias voltage is shown as a function of (a) atomic ratio of Co/Gd, (b) atomic ratio of Co/Mo, and (c) atomic percent of Ar. Data point symbols are defined in Fig. 1.

the target and substrate impedances. Unless otherwise indicated, film thicknesses are in the range $\frac{1}{4} \mu m$ to $2 \mu m$. Over this range, the film properties are essentially independent of film thickness. The rate of deposition increases monotonically with Ar gas pressure, ranging between 190 and 300 Å/min for the indicated pressures. At constant pressure, the film thickness can be precisely controlled by the sputtering time. The lowest achievable pressure in this system is 10^{-8} Torr, obtained by means

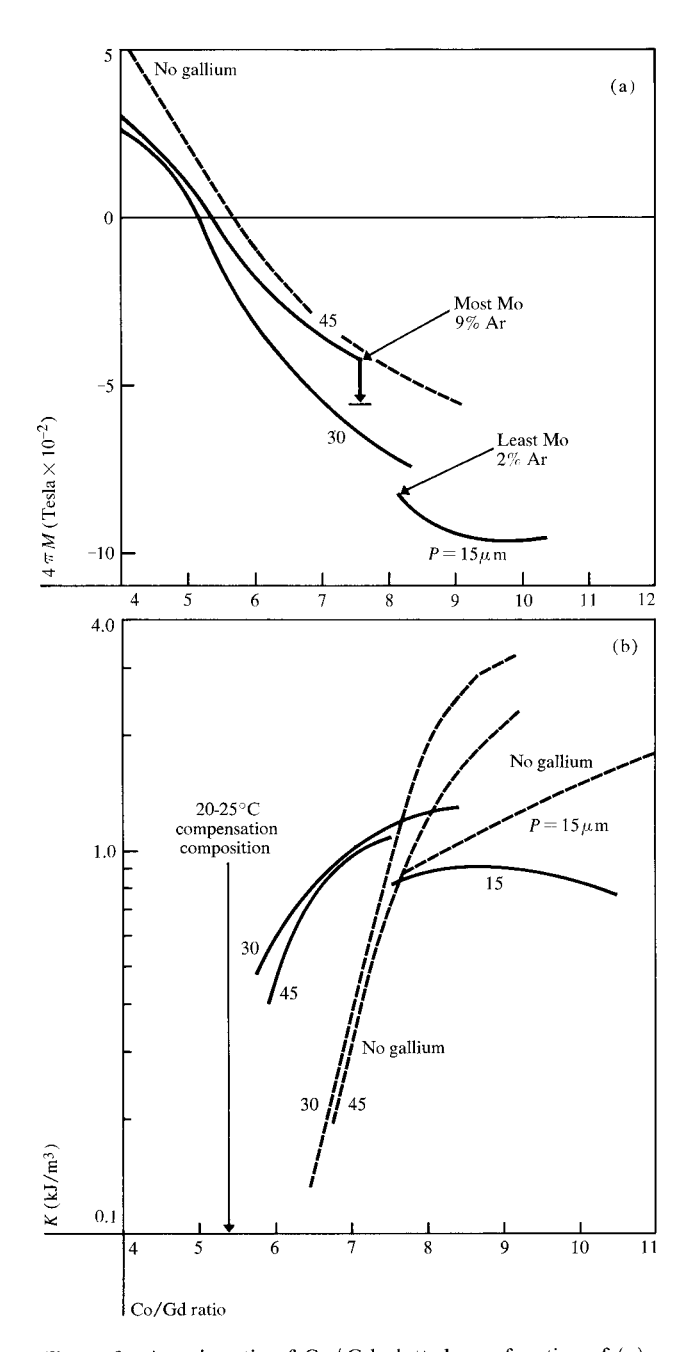


Figure 3 Atomic ratio of Co/Gd plotted as a function of (a) magnetization and (b) anisotropy energy. The heavy arrow in (a) represents the estimated change of magnetization caused by dilution due to excess of Mo and Ar gas (see text).

of oil diffusion and Ti sublimation pumps. However film properties are insensitive to background pressures as high as 10^{-6} Torr.

The effective anisotropy, H_k^* , corresponding to the data of Fig. 1(a), deduced from the in-plane hysteresis loops measured with a 60-Hz, 0.25-T (2.5-kG) peak inductive magnetometer is plotted in Fig. 1(b). In films with a large perpendicular anisotropy \lceil data shown in

Fig. 1(b)], these are hard-axis loops exhibiting a well-defined saturation breakpoint on the M vs H loops, defined as H_k^* .

Incidentally, the square data points of Figs. 1(a) and 1(b) correspond to film properties duplicated from the same target at 3×10^{-2} Torr of Ar in a second sputtering system designed to have the same geometry, pressure, and voltages as those used in this investigation. This exemplifies the degree of intersystem reproducibility achievable by controlling these basic parameters.

Figures 2(a), 2(b) and 2(c) display film composition vs substrate bias voltage. In Figs. 2(a) and 2(b) this information is conveniently plotted in terms of ratios of atomic fractions.

In an assessment of the information in Figs. 1 and 2, it should be emphasized that varying the substrate bias voltage at fixed target voltage changes the film composition relative to that of the target. This change is largest for Gd. The film composition also depends strongly on Ar gas pressure. This dependence is to be expected in sputtering from multicomponent targets with geometries of finite aspect ratio, i.e. the ratio of target diameter to the target-to-substrate distance. Different elements have dissimilar sputtering yields, sticking coefficients, and losses due to scattering in the plasma [30]. Although such mechanisms can explain the observed results, at present there is no model that can quantitatively predict the observed properties from first principles.

The same sputtering geometry factors that lead to the variation of composition with sputtering parameters can produce film property nonuniformities. The horizontal dashed line of Fig. 2(a) represents a film composition equal to that of the target. To rf bias sputter this composition would require an infinite aspect ratio and therefore would produce perfectly uniform films. In practice, film uniformity over realistic substrate dimensions, e.g., 10 cm, might be realized with targets of diameters of 25 to 40 cm [27].

At present these composition dependences on voltage and pressure are useful for investigating film properties over substantial composition ranges from one target. However, as can be deduced from Figs. 1 and 2, reproducible film properties require stringent control of gas pressure and rf voltages. This can be readily achieved by means of feedback control of the voltages to \pm one percent and the Ar gas pressure to $\pm 0.25 \times 10^{-3}$ Torr. Table 2 exemplifies typical reproducibility results for films from seven consecutive depositions with fixed processing parameters. Note that the stripe collapse field for the fourth deposition is anomalously high.

Film composition, properties and, hence, reproducibility also depend on substrate mounting details. Figures 1 and 2 compare the properties of films deposited on substrates with and without gallium backing to the Mo

substrate holder. Backing is expected to reduce the surface temperature of substrates during deposition, although it may also alter the substrate impedance and thus modify the electric potential at the substrate surface. At present it is not clear which of these effects predominates. Nevertheless the interface between substrate and holder requires special attention to achieve desired as well as reproducible properties [29].

Figure 2(c) shows the percentage of Ar gas included in the films by means of the sputtering process. It can be as high as 10 at.% at -160 V, as is often required to achieve bubble domain films. The role of Ar in the film is not fully understood. Annealing experiments and chemical analysis suggest that it is retained in the films after short exposures to 350° C [30].

The magnetization and anisotropy energy vs Co/Gd ratio deduced from the curves in Figs. 1 and 2 are plotted in Figs. 3(a) and 3(b). The values of the anisotropy energy density K are deduced from the relation $H_k^* = 2K/M$. Ferromagnetic resonance [31] and torque magnetometry measurements [32] with films in a single domain state confirm that in the thickness and domain size ranges under consideration H_k^* is an accurate $(\pm 10\%)$ measure of H_k .

The arrow in Fig. 3(a) represents the estimated change of magnetization caused by dilution due to excess Mo and Ar in the films deposited at 45 μ m of Ar pressure. Note that, as expected, with the exception of small corrections to account for those differences in the Mo and Ar contents, the data suggest that the magnetization primarily depends on film composition and not the sputtering process per se, whereas the anisotropy energy density K exhibits a more complex behavior. For instance, compare the curves of Fig. 3(b) corresponding to gallium backed and unbacked samples.

The processing factors that influence K are poorly understood. As reviewed by Vossen [29], properties of sputtered films depend strongly on a multiplicity of interdependent effects related to target and film composition, target and substrate potentials and temperatures, sputtering gas pressure, substrate bombardment by various energetic species, gaseous inclusions, etc. Attempts to vary deposition conditions to separate these effects suggest that although K appears to correlate well with some of these variables over limited ranges, no definite correlation has yet withstood close scrutiny over a broad data base. Understanding of these effects is essential for the ultimate achievement of optimum film properties.

The stability factor $Q = K/2\pi M^2$ as a function of substrate bias voltage is illustrated in Fig. 4 for an argon pressure of 3×10^{-2} Torr. The vertical line at -55 V denotes the 25°C compensation composition (M = 0). This behavior is typical for this class of film materials. The numerals 0.5, 1, and 2 denote room-temperature

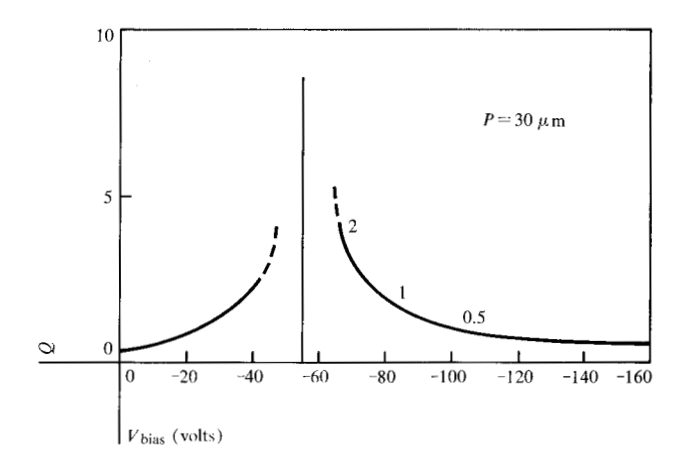


Figure 4 Relation of stability factor Q to substrate bias voltage.

Table 2 Some data showing reproducibility of amorphous films, sputtered in Ar, for seven consecutive deposits with fixed processing parameters.

Stripe width $W_{_8}(\mu\mathrm{m})$	Stripe collapse field $H_{\rm se}(10^4{ m A/m})^{ m a}$	
0.87	4.170	
0.83	4.249	
0.88	4.074	
0.87	4.631	
0.80	4.170	
0.82	4.249	
0.81	4.090	
Average: 0.84	4.233	
Std. dev.: 0.03	0.112	

 $^{^{}a}$ 1.0 oe = 79.577 A/m

bubble diameters in micrometers. This result suggests that although K is large near compensation, it does not allow for attainment of arbitarily large Q values for films with large magnetizations. The implications and generality of this result are discussed in the next section. It is often equally easy to "tune" desired bubble diameters on both sides of the compensation point. However the temperature dependence is usually too pronounced in films having a compensation temperatures above room temperature.

Films deposited in this manner have been successfully used to implement experimental T-I bar devices with bubble diameters of 2 μ m [2]. With the exception of a much larger temperature sensitivity, their operating characteristics are remarkably similar to those of equivalent garnet-based devices. The use of 12-cm targets readily allows for deposition on seven substrates 2.5 cm in diameter with wafer-to-wafer and run-to-run reproducibilities better than five percent. The uniformity of properties is adequate to implement arrays of devices

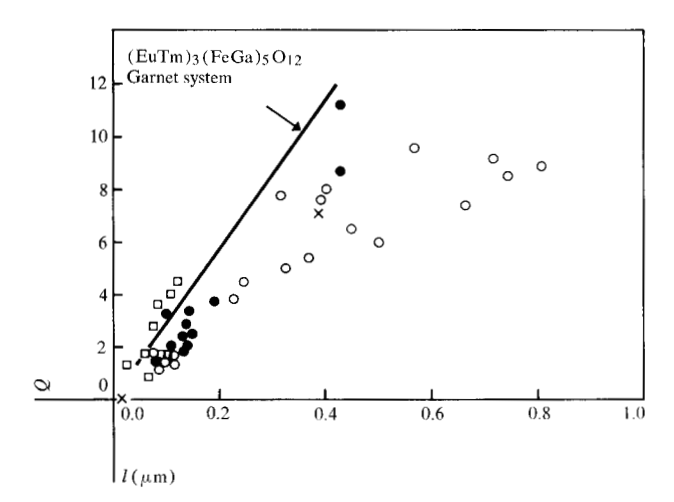


Figure 5 Relation of stability factor Q to characteristic material length l for a garnet system, compared with four different amorphous films. Plotted points are for Gd-Co-Mo films with different Mo contents (open circles, 12 percent; squares, 15 percent; and solid circles, 17 percent) and for Gd-Co-Au films $(\times, 10 \text{ percent Au})$.

with excellent overlaps of operating margins over 2×2 cm of each of the seven substrates [2].

Representative film properties: comparison with garnets

◆ Stability factor Q

Attainment of stable but stationary bubbles in a film usually requires that $Q = H_k/4\pi M \gtrsim 1$. However, as pointed out in the section on submicrometer physics and also in a recent investigation of nucleation in T-I bar type devices, reliable propagation of bubbles without spurious nucleation due to the driving fields from the magnetic propagation overlays requires Q's substantially greater than 2.5, most likely in the range 4 to 5 [7]. Consideration of any bubble material thus requires a critical assessment of attaining sufficiently large Q values. In Fig. 5, Q is plotted vs l for several bubble materials: three Gd-Co-Mo alloys with varying content of Mo, limited data for Gd-Co-Au films, and data for one garnet system [33]. Note that Q correlates strongly with l in all cases. In particular note that Q's corresponding to films having a bubble diameter of 0.5 μ m ($l \approx 0.05$) are expected to be only in the range one to two, a marginal value relative to the considerations discussed here. In both types of materials, decreasing l requires increasing the magnetization of the films. This increase is usually accompanied by an increase in anisotropy energy density K; however K does not increase rapidly enough to retain the Q values of larger-l materials. These data also show why previous investigations were not usually concerned with Q. These emphasized bubble diameters in the vicinity of five μ m, where a Q as large as 10 can be readily achieved.

With reference to Eqs. (1) and (2), constant ratios of Q/l imply a constant ratio of A/K (constant domain wall width) for these materials. It is not surprising that this ratio varies slowly for small composition variations, but at present there is no physical basis to support this relationship for large compositional and material variations. The alloys considered in Fig. 5 cover broad ranges (3:1) for the magnetization, anisotropy, and exchange constants at each of the indicated l values. However, the trend is sufficiently clear to warrant future attention to whether film growth conditions can result in larger anisotropies for fixed composition in the small-l materials.

Although these considerations are likely to be critical in T-I bar type devices, it is not clear how these apply to other devices, such as contiguous disk structures and bubble lattice arrays, which employ different means of propagation. Contiguous disk devices use fields from domain walls in capping layers. Lattice arrays generally require conductor-line propagation. Both may lead to stray fields which would not nucleate unwanted domains in materials of lower Q.

• Coercivity and mobility

Although little is known about the specific mechanisms that define coercivity, experience suggests that it could be affected by film parameters such as $H_k, Q, 4\pi M$, proximity to the compensation temperature, surface effects, and defects. At present very limited data exist on coercivity in submicrometer materials.

Figure 6(a) illustrates the coercivity and l parameter for the $(EuTm)_3$ Ga_x Fe_{5-x} O_{12} garnet system as a function of Ga content. The coercivity in all cases was deduced from the zero-M crossings of the perpendicular magneto-optical [34] or Hall effect [35] hysteresis loop for amorphous films and from the perpendicular susceptibility technique [36] for garnet films. Both techniques correlate well and with coercivities deduced from bubble translation experiments. The results clearly suggest that coercivity monotonically decreases with decreasing l parameter, a desirable trend. It is expected to be only a few tenths of an Oersted for submicrometer bubble diameter films. These films were specially grown to have constant l/h ratios, with $w_s = h$. However, it should be noted that changing I requires changing other film properties. Thus the observed trends in H_c may not be related to / per se.

By contrast, measurements in Gd-Co-Mo films show that coercivity is consistently higher than that of typical garnet films, but that it also decreases with decreasing l. Specifically H_c is typically 3-5, 2-3, and 1-2 Oe for films with l = 0.2, 0.1, and 0.05, respectively, approximately

five times higher than that observed in the garnet system of Fig. 6. However the $H_{\rm c}/4\pi M$ values for the amorphous films are only 0.1% for l=0.05, and are not expected to pose any problem for T-I bar type devices in which the predominant term defining the minimum propagation field is due to the magnetization of the film [8, 9]. The higher coercivities could be of concern in other devices.

The coercivity of amorphous films depends on the aspect ratio of the domains (i.e., ratio of stripe width to film thickness) as is illustrated in Fig. 6(b). The aspect ratio was varied by decreasing the sputtering time, and therefore the film thickness, for material of constant l parameter. This behavior could be ascribed to surface effects at the film-substrate and film-ambient interfaces. Resputtering is known to admix substrate and film constituents to depths as great as 500 Å [37]. Exposure of films to atmospheric conditions is known to alter the outer 200 Å of the film because of oxidation [34]. These regions become proportionately larger for thinner films. Oxidation could be easily avoided by passivating the film prior to atmospheric exposure [34]. These results suggest that it may be desirable to use thicker than normal films, $w_s \approx h$, to achieve lower coercivities.

This dependence of coercivity on thickness has also been observed, but not characterized systematically, in garnet films having bubble diameters of 5 to 10 μ m.

In addition to minimizing the coercivity, it is essential to eliminate defect-induced pinning sites. The defect levels in garnet films can be reduced to a few defects per cm² [38, 39]. The minimum defect levels in amorphous films have not yet been determined. The main contributors to defects in amorphous films are the substrate quality and debris on the substrate. There is no fundamental reason why debris cannot be removed from glass substrates, although, as was pointed out in the section entitled "General Considerations," the additional costs involved may justify the use of polished Si substrates.

Defects can also be introduced during the sputtering process by debris dislodged from the target or the system. A sputter-up configuration has been suggested to minimize target debris [16], whereas general system cleanliness will minimize the latter source of defects.

Bubble mobilities in both the amorphous film and garnets have been discussed in the literature [40, 41]. A mobility of 1000 cm/s-Oe has been observed for one- μ m bubbles in EuTm garnets [41]. This can be compared to mobilities in excess of a few thousand cm/s-Oe in amorphous films [41]. The mobilities observed in garnet films are probably adequate for current device designs operating up to one MHz, whereas the higher mobilities of the amorphous material may be of value for higher-data-rate devices. It should be noted, however,

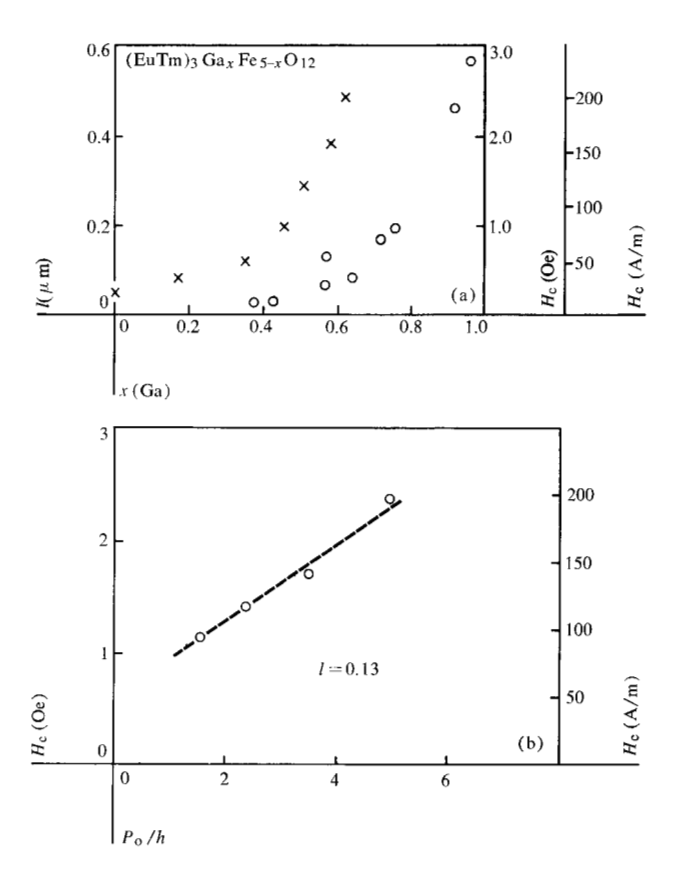


Figure 6 Relation of coercivity to other film parameters. (a) H_c and l vs Ga content for the europium-thulium garnet system. H_c values are open circles and l values are \times s. (b) H_c vs the domain aspect ratio for Gd-Co-Mo films of constant l. $(P_0 = 2w_s)$.

that achievable mobilities in both materials may require reassessment if Q is substantially increased over present values, since the mobility is inversely proportional to Q [42].

• Film stability and temperature sensitivity

Processing and packaging constraints suggest temperatures as high as 250°C. Most devices utilize Permalloy features for propagation elements and magnetoresistive detectors. The maximum safe temperature for Permalloy is in the vicinity of 300°C.

Neither limit is expected to be of concern for garnet films; however, even 250°C may be excessive for amorphous films. Gd-Co-Mo films have been shown to change magnetic properties measurably at annealing temperatures as low as 200°C [30]. The significance of this sensitivity to annealing will depend on whether such changes are reproducible and accompanied by the retention of adequate magnetic properties. The films could thus be stabilized by preannealing at a temperature greater than the maxima expected from realistic processing and packaging. To date, many devices have been success-

fully fabricated on amorphous Gd-Co, Gd-Co-Au, and Gd-Co-Mo films without such a preannealing step. However, this factor remains to be carefully assessed.

It has been shown in the discussion determining the optimum amorphous film composition that it is possible to obtain good temperature-insensitive behavior in the magnetic properties of amorphous films. Similarly, any garnet film composition that exhibits a large exchange stiffness (high Curie temperature), and does not contain ions which produce magnetic compensation near room temperature (e.g., Gd), leads to temperature-insensitive behavior. For example, Gd-Co-Mo films designed to have bubbles 0.9 µm in diameter have been found to show a 20 percent increase in stripe collapse field and a 20 percent decrease in stripe width over a range of 0° to 100°C [43], and (EuTm)₃(FeGa)₅O₁₂ garnet films with 1.0-\mu m diameter bubbles have shown decreases of 20 and 4 percent for stripe collapse field and stripe width, respectively, over a range of 20° to 130°C [44].

Another related issue that warrants consideration in amorphous films is corrosion. In principle, it should be possible to hermetically seal any device. In practice, there will always be defects which, in devices based on amorphous films, could permit corrosion of the storage layer in addition to corrosion of the conductor and propagation overlays.

Summary and conclusions

We have outlined general considerations dictated by device requirements for defining micrometer and sub-micrometer amorphous bubble device materials. Attainment of these characteristics requires optimizing the growth process and composition of the films. We have described the growth processes and specifications necessary for achieving better than five percent reproducibility of film properties in amorphous materials.

A comparison of equivalent garnet and amorphous films reveals that materials made to date have very comparable properties except for considerably larger, but not necessarily prohibitive, coercivities in Gd-Co-Mo films.

Application of either material to submicron T-I bar devices depends on achieving sufficiently large Q values. Future device and material investigations are expected to lead to establishment of minimum acceptable Q values, as well as means for achieving larger anisotropies in these films.

Dielectric breakdown, corrosion, and sensitivity to annealing at relatively low temperatures are key factors that may limit application of the amorphous films. Accepting these deficiencies will require establishing clear superiority over garnets in factors such as higher mobility, lower processing cost, larger substrate areas, and lower defect levels. In amorphous films further work is required to establish how sputtering parameters, especially geometry, influence uniformity. The use of rotating substrate holders can improve the uniformity of films sputtered from arcmelted targets, but associated with the rotating holder is the difficulty of controlling substrate temperature. Recent results, however, show that hot-pressed targets do not require substrate rotation, and thus the temperature of the substrate holders can be controlled adequately. Substrate temperature is expected to influence film properties and, when precisely varied, could result in higher anisotropies and therefore higher Q values.

Acknowledgments

We are grateful for the assistance of E. A. Giess, D. E. Cox, S. Ellman, R. J. Gambino, V. Gilligan, C. F. Guerci, J. Kuptsis, V. Ranieri, V. Richardson, and P. Silano in various aspects of this investigation and we thank Carol Hand for preparation of the typescript.

References

- L. L. Rosier, "Overview of Magnetic Bubble System Development," presented at the INTERMAG Conference, London, 1975, paper no. 32-5.
- M. H. Kryder, K. Y. Ahn, and J. V. Powers, "Amorphous Film Magnetic Bubble Domain Devices," presented at the INTERMAG Conference, London, 1975, paper no. 6-3.
- 3. J. E. Davies and E. A. Giess, "The Design of Single Crystal Materials for Magnetic Bubble Applications," J. Materials Sci., to be published.
- J. M. Robertson, W. Tolksdorf, and M. D. Jonker, "Growth Mechanisms and Composition in the LPE Process for Bubble Domain Materials," J. Cryst. Growth 27, 337 (1974)
- A. A. Thiele, "The Theory of Cylindrical Magnetic Domains," Bell System Tech. J. 48, 3287 (1969).
- A. A. Thiele, "Theory of the Static Stability of Cylindrical Domains in Uniaxial Platelets," J. Appl. Phys. 41, 1139 (1970).
- M. H. Kryder, C. H. Bajorek, and R. J. Kobliska, IEEE Trans. Magnetics, to be published.
- P. K. George, A. J. Hughes, and J. L. Archer, "Submicron Bubble Domain Device Design," *IEEE Trans. Magn.* MAG-10, 821 (1974).
- M. H. Kryder, K. Y. Ahn, G. S. Almasi, G. E. Keefe, and J. V. Powers, "Bubble to T-I Bar Coupling in Amorphous Film Small Bubble Devices," *IEEE Trans. Magn.* MAG-10, 825 (1974).
- R. Wolfe, J. F. Fischer, W. A. Johnson, R. R. Spiwak, L. J. Varniein, and R. F. Fischer, "Ion Implanted Patterns for Magnetic Bubble Propagation," 18th Annual Conference on Magnetism and Magnetic Materials, Denver, AIP Conf. Proc., No. 10, 339 (1973).
- O. Voegeli, B. A. Calhoun, J. C. Slonczewski, and L. L. Rosier, "The Use of Bubble Patterns for Information Storage," 20th Annual Conference on Magnetism and Magnetic Materials, San Francisco, AIP Conf. Proc., No. 24, 617 (1975), as well as other papers in same conference session.
- F. C. Rossol, "Temperature Dependence of Rare-Earth Orthoferrite Properties Relevant to Propagating Domain Device Applications," *IEEE Trans. Magn.*, MAG-5, 562 (1969).

- 13. S. I. Tan, K. Y. Ahn, N. G. Ainslie, and A. F. Mayadas, Dielectric Integrity in Amorphous Film Bubble Devices, presented at the INTERMAG Conference London, 1975, paper no. 6-4.
- 14. P. Chaudhari, J. J. Cuomo, and R. J. Gambino, "Amorphous Bubble Domain Materials," IBM J. Res. Develop. 17, 66
- 15. R. J. Gambino, P. Chaudhari, and J. J. Cuomo, "Amorphous Magnetic Materials," 19th Annual Conference on Magnetism and Magnetic Materials, Boston, AIP Conf, Proc., No. 18, 578 (1973).
- 16. P. Chaudhari, J. J. Cuomo, R. J. Gambino, and E. A. Giess, Physics of Thin Films, R. W. Hoffman, Ed., vol. 8, Academic Press, New York, 1974.
- 17. P. Chaudhari, J. J. Cuomo, R. J. Gambino, S. Kirkpatrick, and L. J. Tao, "Ternary Amorphous Alloys for Bubble Domain Applications," 20th Annual Conference on Magmetism and Magnetic Materials, San Francisco, AIP Conf. Proc., No. 24, 562 (1975).
- 18. J. W. Schneider, "Amorphous Gd-Co-Cr Films for Bubble Domain Applications," IBM J. Res. Develop. 19, 587 (1975).
- 19. T. Kobayashi, N. Imamura, and Y. Mimura, "Magnetic Properties of GdFe Amorphous Alloy Films Prepared by Sputtering," 20th Annual Conference on Magnetism and Magnetic Materials, San Francisco, AIP Conf. Proc., No. 24, 566(A) (1975).
- 20. H. C. Bourne, Jr., R. B. Goldfarb, W. L. Wilson, Jr., and R. Zwingman, "Effect of DC Bias on the Fabrication of Amorphous GdCo RF Sputtered Films," presented at the INTERMAG Conference, London, 1975, paper no. 31-8.
- 21. R. Hasegawa, B. E. Argyle, and L-J. Tao, "Temperature Dependence of Magnetization in Amorphous Gd-Co-Mo Alloys," 20th Annual Conference on Magnetism and Magnetic Materials, San Francisco, AIP Conf. Proc., No. 24, 110 (1975).
- 22. R. Hasegawa, "Temperature and Compositional Dependence of Magnetic Bubble Properties of Amorphous Gd-Co-Mo Films," J. Appl. Phys. 46, 5263 (1975).
- 23. R. Hasegawa and R. C. Taylor, "Magnetization of Amorphous Gd-Co-Ni Films," J. Appl. Phys. 46, 3606 (1975).
- 24. Kenneth Lee and Neil Heiman, "Magnetism in Rare Earth-Transition Metal Amorphous Alloy Films," 20th Annual Conference on Magnetism and Magnetic Materials, San Francisco, AIP Conf. Proc., No. 24, 108 (1975).
- 25. F. B. Hagedorn, "Anisotropy in Garnet Films," 7th International Colloquium on Magnetic Films, Regensburg, West Germany, 1975.
- 26. M. Hansen, Constitution of Binary Alloys, McGraw-Hill Book Company, Inc., New York, 1958.
- 27. R. J. Kobliska, R. Ruf, and J. Cuomo, "Uniformity of Amorphous Bubble Films," 20th Annual Conference on Magnetism and Magnetic Materials, San Francisco, AIP Conf. Proc., No. 24, 570 (1975)
- 28. L. Maissel, Handbook of Thin Film Technology, L. Maissel and R. Glang, eds., McGraw-Hill Book Company, Inc., New York, 1970, ch. 4.
- 29. J. L. Vossen, "Control of Film Properties by RF Sputtering Techniques," J. Vac. Sci. and Technol. 8, 512 (1971).

- 30. R. J. Kobliska and A. Gangulee, "Annealing Behavior of Amorphous Gd-Co-Mo Thin Films," 20th Annual Conference on Magnetism and Magnetic Materials, San Francisco, AIP Conf. Proc., No. 24, 567 (1975).
- 31. As determined by C. H. Bajorek and P. Chaudhari.
- 32. As determined by C. H. Bajorek and C. H. Wilts.
- 33. E. A. Giess, J. E. Davies, C. F. Guerci, and H. L. Hu, "Gallium Concentration Effects on Magnetic Bubble Films on EuTm₂(FeGa)₅O₁₂ Garnet Grown by LPE," Mtls. Res. Bull., 10, 355 (1975).
- 34. B. E. Argyle, R. J. Gambino, and K. Y. Ahn, "Polar Kerr Rotation and Sublattice Magnetization in Gd-Co-Mo Bubble Films," 20th Annual Conference on Magnetism and Magnetic Materials, San Francisco, AIP Conf. Proc., No. 24, 564 (1975).
- 35. K. Okamoto, T. Shirakawa, S. Matsushita, and Y. Sakurai, "Hall Effect in Gd-Co Sputtered Films," IEEE Trans. Magn. MAG-10, 799 (1974).
- 36. P. W. Shumate, D. H. Smith, and F. B. Hagedorn, "The Temperature Dependence of the Anisotropy Field and Coercivity in Epitaxial Films of Mixed Rare-Earth Iron Garnets," *J. Appl. Phys.* **44**, 499 (1973). 37. P. Ho, K. Ahn, and C. H. Bajorek, to be published.
- 38. J. W. Nielsen, S. J. Licht, and C. D. Brandle, "The Preparation of Large Area Films for Bubble Domain Devices,' IEEE Trans. Magn. MAG-10, 474 (1974).
- 39. B. S. Hewitt, R. D. Pierce, S. L. Blank, and S. Knight, "Technique for Controlling the Properties of Magnetic Garnet Films," IEEE Trans. Magn. MAG-9, 366 (1973).
- 40. H. L. Hu and E. A. Giess, "Dynamics of Micron Size Bubbles," 20th Annual Conference on Magnetism and Magnetic Materials, San Francisco, AIP Conf. Proc., No. 24, 605 (1975).
- 41. M. H. Kryder and H. L. Hu, "Bubble Dynamics in Amorphous Magnetic Materials," 19th Annual Conference on Magnetism and Magnetic Materials, Boston, AIP Conf. Proc. No. 18, 213 (1973).
- 42. U. F. Gianola et al., "Material Requirements for Circular Magnetic Domain Devices," IEEE Trans. Magn., MAG-5, 588 (1969)
- 43. R. J. Gambino et al., Proceedings of the International Conference on Magnetic Bubbles, Eindhoven, Netherlands, September 1976, to be published.
- 44. E. A. Giess, J. E. Davies, C. F. Guerci, H. L. Hu, J. D. Kuptsis, and J. M. Shaw, "(EuTm)₃(FeGa)₅O₁₂ Garnet Films with One-Micron Diameter Magnetic Bubbles,' 20th Annual Conference on Magnetism and Magnetic Materials, San Francisco, AIP Conf. Proc., No. 24, 582 (1975).

Received May 27, 1975; revised November 10, 1975

The authors are located at the IBM Thomas J. Watson Research Center, Yorktown Heights, New York 10598.